2021 43rd Annual International Conference of the
IEEE Engineering in Medicine & Biology Society (EMBC)
Oct 31 - Nov 4, 2021. Virtual Conference

Acoustic Bruit Transduction Interface for Non-Invasive Vascular Access Monitoring

Rohan K. Sinha, *Member, IEEE,* Hossein Miri Lavasani, *Senior Member, IEEE,* Christian Zorman, *Senior Member, IEEE* and Steve J.A. Majerus, *Senior Member, IEEE*

***Abstract*— Hemodialysis is a treatment for patients suffering from chronic or acute kidney disease, and is administered via an arteriovenous vascular access. One symptom of a dysfunctional vascular access are blood sounds (bruits) produced by turbulent flow. This paper discusses the design and characterization of a multichannel transducer array to capture blood sounds from multiple sites simultaneously. Recorded sounds can be classified by digital signal analysis to categorize severity of dysfunction based on acoustic features. Using a vascular access phantom with 5-80% degree of stenosis and blood mimicking fluid flowing at a rate of 850-1200 mL/min, we analyzed the acoustic properties of blood sounds recorded from a flexible microphone transducer. The signal bandwidth (2.25 kHz) and the dynamic range (60.2 dB) were determined, allowing optimization of a transimpedance transducer interface amplifier.**

***Clinical Relevance*—Vascular access stenosis causing turbulent flow produces bruits with spectral content related to degree of stenosis. A flexible microphone recording array could be used for point-of-care monitoring of vascular access function.**

I. Introduction

Patients suffering from end stage renal disease are frequently treated using hemodialysis [1] wherein arterial blood is filtered through a dialyzer and returned to the venous system. Efficient dialysis requires high rates of blood flow, so typically a surgically-created vascular access is created using an arteriovenous fistula/graft. (Fig. 1)

Clinical monitoring is used to estimate when a vascular access is no longer supporting enough blood flow or is at risk for clotting or thrombosis. Daily and weekly monitoring relies on physical examination, including the use of a stethoscope to listen to sounds of blood flow. Doppler duplex ultrasound requires equipment and trained personnel to interpret results; as a result, it is too costly for regular monitoring [2]. Physical examination via stethoscope has reasonable diagnostic accuracy, but is confounded by the skill of the examiner, how often the examination is performed, and limited quantitative record [3].

Blood sounds (bruits) arise from velocity fluctuations within vessels. The presence of a stenosis results in turbulent flow and pressure fluctuations in the vessel wall near the site of occlusion [4]. This phenomenon results in very distinct bruits which are easily heard via stethoscope. Other published work demonstrates a level of predictability in the effect stenoses have on bruits [5]. Recording and analyzing these bruits—phonoangiography—allows quantitative description of bruits. Phonoangiography is a potentially cheaper and more accessible monitoring strategy which can augment physical examination of vascular access via stethoscope.

We previously described flexible microphone arrays for vascular access phonoangiography [5], and in this work we analyze the essential bandwidth and dynamic range of the front-end interface amplifiers and data converters needed to capture phonoangiograms (PAGs). Next, we describe how recording arrays enable time-, spectral-, and spatial-domain features to be extracted from PAGs.

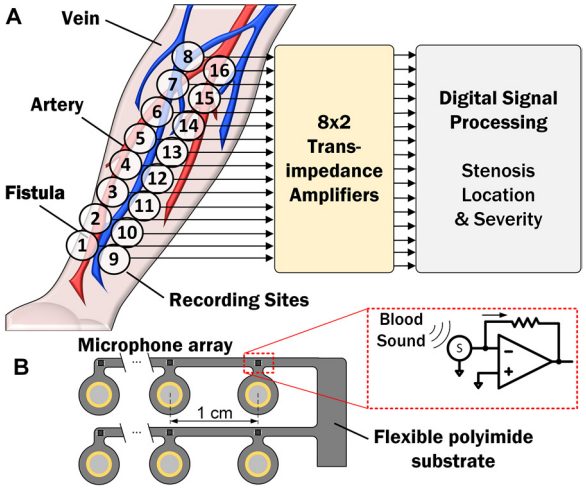

Figure 1. (a) An 8x2 array samples data from 16 sites along the vascular access for amplification and signal processing. (b) The array is built from a flexible material with each sensor 1cm apart for maximum contact. A transimpedance interface amplifier is housed on the board as well for amplification immediately after a signal is generated.

II. Transducer Interface and Design Considerations

A. Skin-coupled microphone array for bruit transduction

The sensing of bruits is accomplished using a thin, flexible microphone array consisting of 2-mm polyvinylidene fluoride (PVDF) diaphragms coated in silicone rubber and mounted to a polyimide substrate [5]. The small size and flexibility of the microphones enables good contact with the skin over the non-

This work was supported in part by RX001968-01 from the US Department of Veteran Affairs Rehabilitation Research and Development Service, the Advanced Platform Technology Center of the Louis Stokes Cleveland VA Medical Center, and by Case Western Reserve University. The contents do not represent the views of the US Government.

R. Sinha, H. M. Lavasani, and C. Zorman are with the Department of Electrical, Computer & Systems Engineering, Case Western Reserve University, Cleveland, OH, 44106, USA.

C. Zorman and S. Majerus are with the Advanced Platform Technology Center, Louis Stokes Cleveland Veterans Affairs Medical Center, Cleveland, OH, 44106, USA (e-mail: steve.majerus@va.gov)

flat anatomy of a vascular access. The films are arranged into an 8x2 array, allowing for PAGs to be recorded from 16 separate locations simultaneously. The flexible polyimide substrate contains integrated front-end interface amplifiers

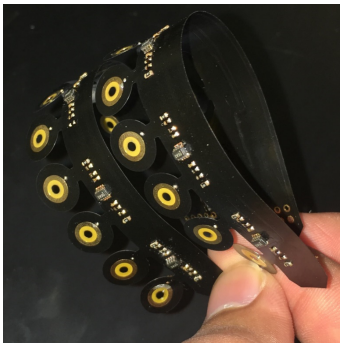

Figure 2. 8x2 array of microphones channels on a flexible polyimide board for housing the PVDF microphones and dedicated transimpedance amplifier stages

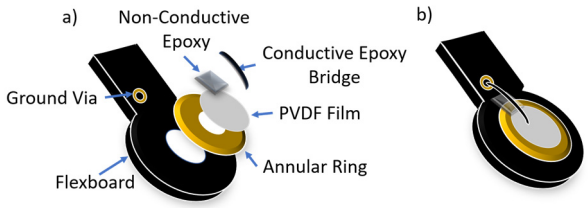

Figure 3: Cross sectional representation of PVDF films, annular ring, and epoxy layers for transduction of bruits. (a) Exploded cross sectional view. (b) Reconstructed view of microphone.

placed near each electrode to amplify the signal provide signal buffering (Fig. 2). After solder reflow assembly of the amplifiers, PVDF microphones were created by attaching cut PVDF films to annular electrodes with conductive epoxy (CW2400, M.G. Chemicals). The same epoxy was used to create a bridge between the top plate of the PVDF film and a nearby ground contact (Fig. 3). A nonconductive epoxy (E-60NC) island was created along the edge of the PVDF film. The conductive epoxy bridge was applied over this island to prevent a connection between the two sides of the film forming at the edge.

B. Noise Current and Bandwidth Optimization

Each microphone in the sensor array was coupled to an interface amplifier to increase the signal amplitude and limit the noise bandwidth. The amplifier noise floor and bandwidth constraints were derived from the PAG signal analysis, while the amplifier gain was optimized for the impedance of the 2-mm PVDF microphone. The sensor's impedance was measured (Hioki IM3570), and each PVDF microphone was modeled as a current source with a parallel capacitor and resistor representing its parasitic properties (Table II).

TABLE II: MEASURED CHARACTERISTICS OF PVDF TRANSDUCERS

Modeled parameter	Value
Current source Amplitude, I_S	$0.63\mu A$
Sensor Resistance, R_S	$12.4\ M\Omega$
Sensor Capacitance, C_S	$100pF$

Since the transducer produces an output current and exhibits a high output impedance, a transimpedance amplifier (TIA) topology was used (Fig. 7).

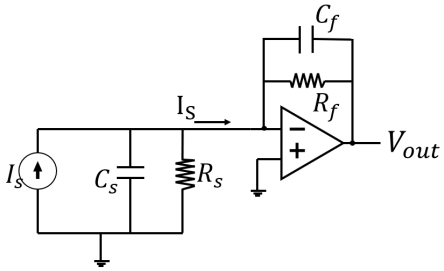

Figure 7. Schematic diagram of a capacitive transducer model interfacing with a transimpedance amplifier. I_S, C_S, and R_S model the PVDF piezoelectric current and equivalent source impedance.

The transimpedance amplifier converts the sensor output current I_S to an output voltage of V_{out} by producing an equal output current which flows through R_f to maintain the inverting input as a small-signal ground. The transimpedance gain (V/A), is set by R_f. Here we used R_f=715 kΩ to produce a 30-mV_{PP} output for the nominal sensor current I_S.

After selecting R_f, the TIA bandwidth, f_{-3dB}, was set by fixing C_f, i.e.

$$C_f = {}^{1}/_{2\pi * R_f * f_{-3dB}}. \quad (1)$$

The large feedback resistor R_f, contributes thermal noise to the TIA. However, there is inherent input-referred noise associated with the op-amp integrated circuit. Determining the appropriate chip to use requires consideration of thermal noise as well as the op-amp's input-referred noise current,

$$i_n = \sqrt{{}^{4kBT}/_{R_f}} + i_{amp\ noise} \quad (2)$$

Where k,B, and T represent the Boltzmann coefficient, the signal bandwidth, and the temperature, respectively. The amplifier bandwidth, B, was selected to be 2.25 kHz as discussed in Section III. The estimated the thermal input noise current is 7.1 pA. The noise current density for the selected op-amp chip (OPA378, Texas Instruments) is 200 $fA/\sqrt{Hz}$ per the datasheet. This is equivalent to an input-referred noise current of 9.5 pA at 2.25 kHz. The total input-referred noise current, the sum of these two currents, is 16.6 pA with an input-referred noise current density of 0.4 $pA/\sqrt{Hz}$. The resulting dynamic range, the designed dynamic range, is 91.6 dB. This designed dynamic range well exceeds the minimum 60.2 dB dynamic range, discussed in Section III, meaning the selected amplifier chip and the amplifier design is sufficient for this application. Optimized TIA circuits (Table III) were soldered to the flexible microphone array near each PVDF microphone.

TABLE III: AMPLIFIER DESIGN PARAMETERS

Minimum dynamic range	60.2 dB
Designed dynamic range	91.6 dB
Nominal sensor output current, I_S	0.63 μA
Transimpedance gain (R_f)	715 kΩ
Nominal output voltage	30 mV_{PP}
Signal bandwidth	2.25 kHz
C_f	100 pF

III. Characterization of Spectral Properties of Phonoangiograms

A. Temporal and spectral analysis of bruits

A pulsatile pumping system comprised of an electronic pump and flow meter (Cole Parmer MasterFlex L/S, Shurflo 4008), and blood mimicking fluid was used to reproduce blood sounds within a vascular access stenosis phantom [5]. Recordings were made 1 cm before stenosis, at the site of stenosis, 1 cm after, and 2 cm after. Degree of stenosis (5 – 80 %) and blood flow rates (850-1200 mL/min) were varied to produce 195 samples for spectral analysis.

Spectral domain analysis of these bruits shows a difference in how signal power and frequency are correlated between sites as well as degrees of stenosis (Fig. 3). While the pulsatile blood flow appears nearly identical in the time domain at 30% and 75% degree of stenosis (Fig. 4a,b), there is a very clear difference in spectral content, making spectral analysis a very valuable tool in any form of PAG investigation. The spectrogram for a 75% degree of stenosis has visibly higher density in higher frequency bands in comparison to the 30% stenosis. This trend forms the basis for the PAG recording and analysis.

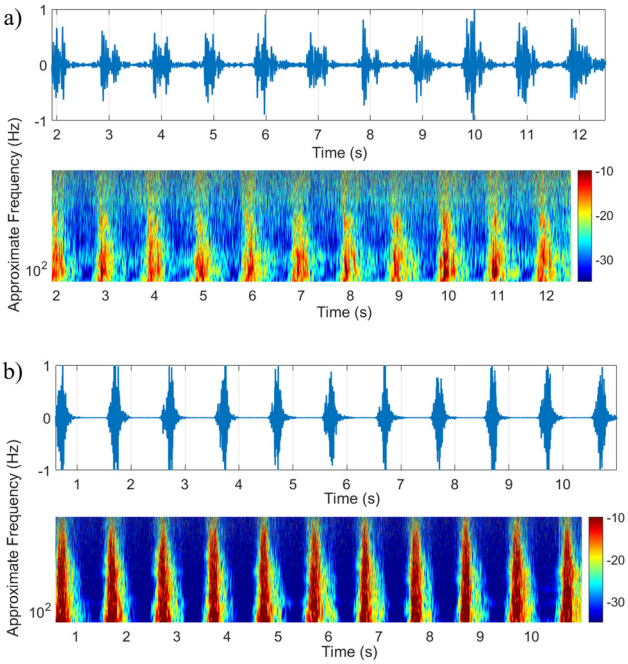

Figure 4. Example temporal and spectral plots of recorded bruit with (a) 30% degree of stenosis and (b) 75% degree of stenosis. The spectrograms show a clear increase in power spectral density at higher frequencies for a higher degree of stenosis

Figure 5 shows the power spectral density of the pulsatile blood flow recorded at the 4 sites as well as a plot of the cumulative sum of spectral power. Sites 1 cm proximal to stenosis generally had higher power spectral density at frequencies below 1 kHz (Fig. 5b, d). Conversely, sites at or after the stenosis, which record sounds of turbulent blood flow as a result of the reduced cross-sectional surface area in the flow path along the vessel, exhibit higher power spectral densities at frequencies above 1 kHz.

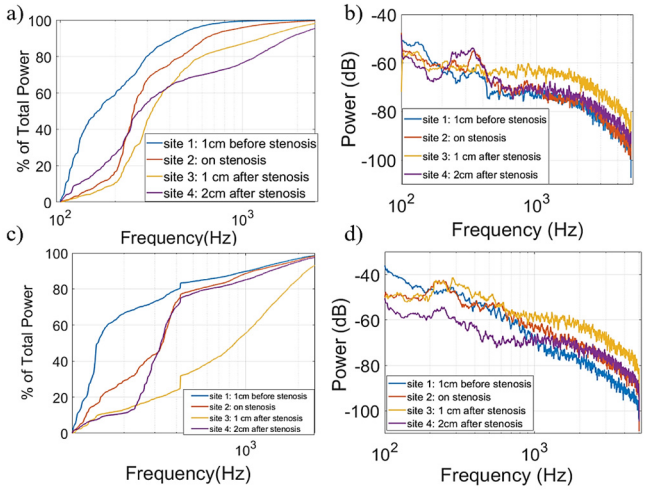

Figure 5. (a) Integrated signal power at each site for 75% degree of stenosis. (b) Power spectral density of 4 sites at 75% stenosis (c) Integrated signal power at each site for 30% degree of stenosis. (d) Power spectral density plot for 4 sites at 30% stenosis. Sites immediately after the stenosis, 1cm and 2cm after, have higher signal power at higher frequencies- a trend consistent at both high and low degrees of stenosis

The difference in spectral bandwidth at each site can be represented using the 95% spectral power threshold. The 95% spectral power threshold is found by computing the cumulative sum of spectral power and dividing it by the total spectral power of the signal. The frequency at which this ratio reaches 0.95 is the 95% threshold. The spectral bandwidth was well above 1 kHz on and after the stenosis with respect to the direction of blood flow, with the highest bandwidth occurring well above 2 kHz (Table I). The quantitative analysis supports the trends from the figures, which suggest an increase in spectral content at higher frequencies at the site of stenosis and 1cm proximal in the direction of blood flow.

TABLE I: 95% SPECTRAL POWER THRESHOLDS AT EACH SITE OF STENOSIS

Position relative to stenosis	95% power threshold at 30% stenosis	95% power threshold at 75% stenosis
1 cm before	1.5 kHz	427.3 Hz
0 cm from stenosis	1.7 kHz	806.9 Hz
1 cm after	2.6 kHz	1.7 kHz
2 cm after	1.9 kHz	2.3 kHz

B. PAG essential bandwidth and dynamic range

Optimizing the analog performance of the front-end amplifier requires determining the dynamic range and essential spectral bandwidth of PAG signals. Previous studies examined these values in PAGs [6]-[15], but used stethoscopes with lower bandwidth than the PVDF microphone. The bandwidth of a stethoscope is insufficient for capturing the full spectral content of blood flow through a stenosed vessel. The essential bandwidth for each signal was calculated by integrating the power spectral density starting at 100 Hz until 95% of the total signal power was reached (Fig. 6). Frequencies below 10 Hz were excluded to reduce the influence of flicker noise. We found that PAGs typically had a bandwidth of 100-1,750 Hz, and selected 2.25 kHz as the maximum required bandwidth for the interface amplifier to

avoid the discrete op-amp's roll off from attenuating any PAG signal content.

PAG minimum dynamic range was calculated as the difference in spectral power from PAGs during the systolic phase of blood flow and the diastolic phase. This method was adopted because the systolic phase of the PAG has higher velocity blood flow and therefore higher acoustic amplitude. Pulse phases were segmented by computing the Shannon energy envelope of the time-domain PAG and setting the segment threshold at the level of the median minus the interquartile range (approximately 25% of the total amplitude). This analysis yielded an average dynamic range of 60.2 dB, or approximately 10-bit quantization accuracy.

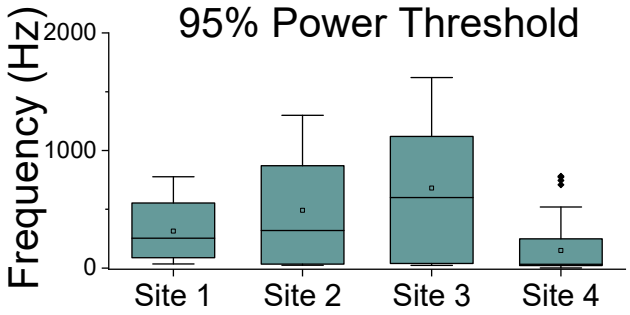

Figure 6. Boxplots of the 95% spectral power threshold at each site in all of the 195 recordings. Site three, corresponding to a position 1cm after the stenosis, has a highest average 95% spectral power threshold- a clear spatial correlation with the presence of stenosis.

IV. Conclusion

Acoustic classification is a method for noninvasive, point-of-care monitoring of vascular accesses. The spectral characteristics of blood flow are affected by the presence of a stenosis and its degree of severity. Higher degrees of stenosis are correlated with higher 95% power thresholds, and at each degree of stenosis, there is a noticeable upward trend in 95% power thresholds at sites on and 1cm proximal to the stenosis. These relationships, when represented quantitatively, form a valid basis for non-invasive acoustic monitoring of a vascular access. Conventional monitoring methods with a stethoscope are cost effective, but lack objectivity and still require coming to a medical center for check-ups. The multichannel data sampling approach described in this paper is able to address both of those issues. The microphone array is able to sample data from multiple locations simultaneously, and generate PAGs necessary for processing just from being fastened on top of the access point. These recordings can be processed for advanced feature extraction to draw conclusions on severity and position of the stenosis. This eliminates the need for a trained medical professional to use a stethoscope and would increase the likelihood that access dysfunction be detected before failure.

References

[1] Flagg, A. J., "Chronic Renal Therapy," *Nursing Clinics of North America,* vol. 53, no. 4, pp. 511-519, Oct. 2018..

[2] Y.-C. C. Du, W.-L. L. Chen, C.-H. H. Lin, C.-D. D. Kan, and M.-J. J. Wu, "Residual stenosis estimation of arteriovenous grafts using a dual-channel phonoangiography with fractional-order features," *IEEE J. Biomed. Heal. Informatics*, vol. 19, no. 2, pp. 590–600, Mar. 2015.

[3] [39] I. Milsom, K. S. Coyne, S. Nicholson, M. Kvasz, C. I. Chen, and A. J. Wein, "Global prevalence and economic burden of urgency urinary incontinence: A systematic review," *European Urology*, vol. 65, no. 1. pp. 79–95, 2014.

[4] Y.-N. Wang, C.-Y. Chan, and S.-J. Chou, "The Detection of Arteriovenous Fistula Stenosis for Hemodialysis Based on Wavelet Transform," *International Journal of Advanced Computer Science,* vol. 1, no. 1, pp.16-22, July 2011.

[5] B. Panda, S. Mandal, S. Member, S. J. A. Majerus, S. Member, and S. J. A. Majerus, "Flexible, Skin Coupled Microphone Array for Point of Care Vascular Access Monitoring," IEEE Trans. Biomed. Circuits Syst., vol. 13, no. 6, pp. 1494–1505, 2019.

[6] H. A. Mansy, S. J. Hoxie, N. H. Patel, and R. H. Sandler, "Computerised analysis of auscultatory sounds associated with vascular patency of haemodialysis access.," *Med. Biol. Eng. Comput.*, vol. 43, no. 1, pp. 56–62, Jan. 2005.

[7] T. Shinzato, S. Nakai, I. Takai, T. Kato, I. Inoue, and K. Maeda, "A new wearable system for continuous monitoring of arteriovenous fistulae.," *ASAIO J.*, vol. 39, no. 2, pp. 137–40.

[8] Yalin Zhang, Qinyu Zhang and Shaohua Wu, "Biomedical signal detection based on fractional fourier transform," 2008 International Conference on Information Technology and Applications in Biomedicine, 2008, pp. 349-352.

[9] I. Clausen, S. T. Moe, L. G. W. Tvedt, A. Vogl, and D. T. Wang, "A miniaturized pressure sensor with inherent biofouling protection designed for in vivo applications," Proc. Annu. Int. Conf. IEEE Eng. Med. Biol. Soc. EMBS, pp. 1880–1883, 2011.

[10] T. Sato, K. Tsuji, N. Kawashima, T. Agishi, and H. Toma, "Evaluation of blood access dysfunction based on a wavelet transform analysis of shunt murmurs," J. Artif. Organs, vol. 9, no. 2, pp. 97– 104, Jun. 2006.

[11] M. Gram et al., "Stenosis Detection Algorithm for Screening of Arteriovenous Fistulae," 15th North-Baltic Conference on Biomedical Enginering and physics, 2011, pp. 241–244.

[12] I. Milsom, K. S. Coyne, S. Nicholson, M. Kvasz, C. I. Chen, and A. J. Wein, "Global prevalence and economic burden of urgency urinary incontinence: A systematic review," European Urology, vol. 65, no. 1. pp. 79–95, 2014.

[13] L. Rousselot, "Acoustical Monitoring of Model System for Vascular Access in Haemodialysis," Ph.D. dissertation, Delft University of Technology, Delft, September, 2014.

[14] S. Gaupp, Y. Wang, T. V How, and P. J. Fish, "Characterisation of vortex shedding in vascular anstomosis models using pulsed doppler ultrasound," *Journal of Biomechanics,* vol. 32, no. 7, pp. 639-645, July, 1999.

[15] R. Gårdhagen, "Turbulent Flow in Constricted Blood Vessels Quantification of Wall Shear Stress Using Large Eddy Simulation," Ph.D. dissertation, Linköping University, Linköping, 2013.